NJC

Tolyporphins A–R, unusual tetrapyrrole macrocycles in a cyanobacterium from Micronesia, assessed quantitatively from the culture HT-58-2

Journal:	*New Journal of Chemistry*
Manuscript ID	NJ-ART-04-2021-002108
Article Type:	Paper
Date Submitted by the Author:	29-Apr-2021
Complete List of Authors:	O'Donnell, Timothy; University of Hawaii at Manoa, Chemistry Gurr, Joshua; University of Hawaii at Manoa, Chemistry Dai, Jingqiu; University of Hawaii at Manoa, Chemistry Taniguchi, Masahiko; North Carolina State University, Department of Chemistry Williams, Philip; University of Hawaii at Manoa, Chemistry Lindsey, Jonathan; North Carolina State University, Chemistry

Tolyporphins A–R,
unusual tetrapyrrole macrocycles in a cyanobacterium from Micronesia,
assessed quantitatively from the culture HT-58-2

Timothy J. O'Donnell,[a] Joshua R. Gurr,[a] Jingqiu Dai,[a]

Masahiko Taniguchi[b,*] Philip G. Williams,[a,*] and Jonathan S. Lindsey[b,*]

[a] Department of Chemistry, University of Hawaii at Manoa, Honolulu, Hawaii 96822-2275, USA

[b] Department of Chemistry, North Carolina State University, Raleigh, NC 27695-8204, USA

mtanigu@ncsu.edu; philipwi@hawaii.edu; jlindsey@ncsu.edu;

ABSTRACT

The 'pigments of life' family has been enlarged by the discovery of the tetrapyrrole macrocycles dubbed tolyporphins, which are present in a cyanobacterial culture (HT-58-2). Of the 18 known tolyporphins, fourteen (A–J and L–O) are dioxobacteriochlorins, three (K, Q and R) are oxochlorins, and one (P) is a porphyrin. The members with a given chromophore absorb similarly but not identically with each other, presenting the problem of absorption spectral aliasing. Tolyporphins G,H are isomers, as are tolyporphins L-O, given the nature of the peripheral (*C*-glycoside, –OH, or –OAc) substituents, presenting the (isobaric) problem of mass spectrometric analysis. The distribution of tolyporphin members is known to change over time and under different growth conditions, yet the complexity of the tolyporphins mixture presents challenges toward characterization of the underlying factors that alter such distributions. Liquid chromatography-mass spectrometry with dynamic multiple reaction monitoring (LC-MS-

dMRM) was employed to characterize the distribution of tolyporphins under distinct growth media, using two semisynthetic standards, tolyporphin A *O,O*-dibutyrate and tolyporphin D *O,O,O,O*-tetrabutyrate. Growth in media containing both ammonium and nitrate salts versus nitrate alone affords increased production of tolyporphins. The absorption spectra of tolyporphins A–R have been reevaluated with regards to molar absorption coefficients, are compared with those of selected tetrapyrrole macrocycles to better understand the effects of chromophores and substituents, and are made available here in print and digital forms for comparison with isolated tolyporphins and mixtures thereof. Together, the work provides the foundation for quantitative assessment of these unusual natural products.

Keywords: Absorption spectra, Bacteriochlorin, Chlorin, Chlorophyll, Cyanobacteria, LC-MS-dMRM, Natural products, Porphyrin

INTRODUCTION

A wide search for neoplastic agents from microbial sources was carried out around 1990 by a team at the University of Hawaii.[1] The search focused on cyanobacteria chiefly located on islands in the Pacific and South Pacific Ocean. Samples were returned to University of Hawaii, grown in culture, and extracts therefrom were subjected to diverse biological assays. This strategy led to the discovery of tolyporphin A, a tetrapyrrolic macrocycle, from the culture HT-58-2.[2] The structure of tolyporphin A is shown in Chart 1, along with that of chlorophyll *a*. Tolyporphin A contains two *C*-glycosides; each *C*-glycoside is attached along with a methyl group at the carbon adjacent to the keto group. The resulting structure is a gem-dialkyl unit,[3] which renders the dioxobacteriochlorin chromophore resistant to adventitious dehydrogenation and to keto-enol tautomerism. Other noteworthy structural features are the two unsubstituted β-pyrrole sites and the free base macrocycle.[4,5]

The absorption spectrum of tolyporphin A is shown in Figure 1, along with that of chlorophyll *a* (both in methanol). Tolyporphin A exhibits a sharp and strong long-wavelength absorption band, known as the Q_y band, at 676 nm. The sharpness of the band is characterized by the full-width-at-half-maximum (fwhm), which here equals 8 nm. The Q_y band of chlorophyll *a* also is quite intense, but at slightly shorter wavelength (665 nm) and with somewhat larger fwhm, of 25 nm. Tolyporphin A and chlorophyll *a* both exhibit a strong absorption (B band) in the near-ultraviolet region, with respective fwhm of 22 and 87 nm.[5,6] The overlap of the absorption band of tolyporphin A with that of chlorophyll *a* prompts numerous questions concerning possible physiological function of tolyporphin A in its native culture, which is now known to be a non-axenic cyanobacterial–microbial holobiont.[7,8] While the native physiological functions of tolyporphins are unknown, experiments *in vitro* have suggested efflux-pump inhibition activity against cancer cells.[9,10] Also, tolyporphin A is photoactive,[11] with excited-state properties typical of tetrapyrrole macrocycles.[6]

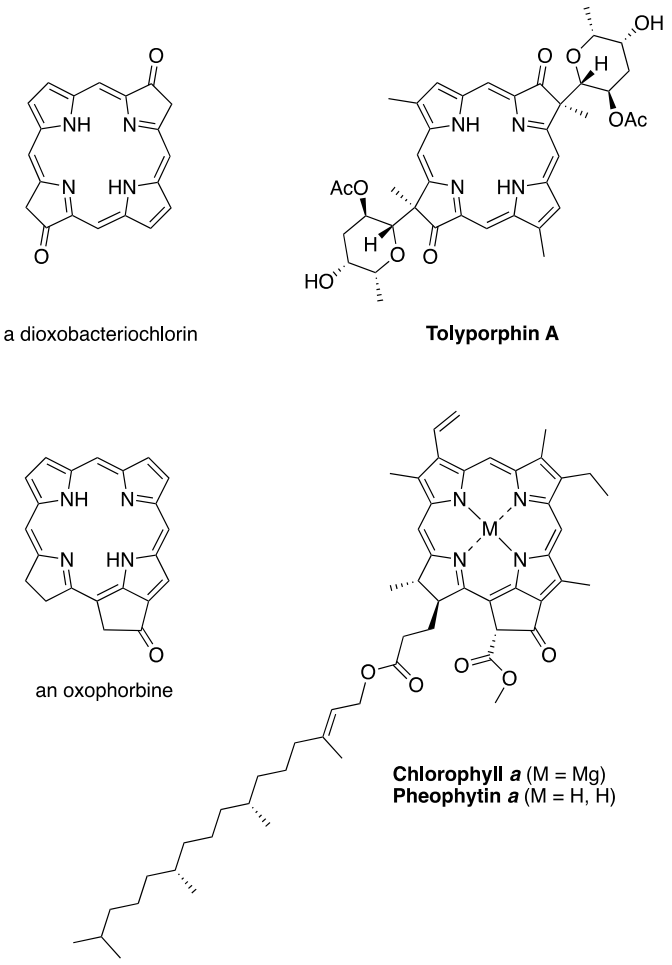

Chart 1. Tolyporphin A and chlorophyll *a*, along with the skeletal chromophores for comparison.

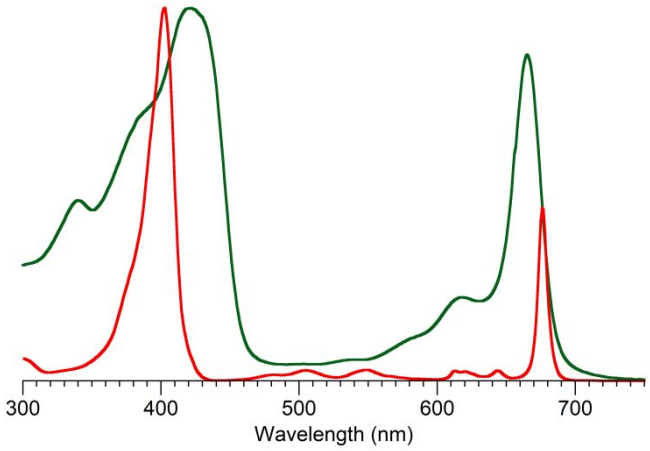

Figure 1. Absorption spectra (normalized) in methanol at room temperature of tolyporphin A (red) and chlorophyll *a* (green).

Subsequent studies over the years of lipophilic extracts of the HT-58-2 culture have led to the identification of a family of tolyporphins, now listed as tolyporphins A–R. The reports include tolyporphins B–I,[12] J and K,[13] and L–R.[14] The structures of tolyporphins A–R are shown in Chart 2. The stereochemical configuration of substituents in the pyrroline rings is uncertain except for that of tolyporphins A, E and R, for which single-crystal X-ray structures have been reported.[14] The various tolyporphins have been noted in a number of reviews.[4,15-19] The presence of a family of tolyporphins is characteristic of natural products biosynthesis but at odds with the typical role of tetrapyrroles as singular products of biosynthesis and function as cofactors in enzymatic and related biological processes.[5]

The study of the distribution of tolyporphins is challenging if not fraught. Chromatographic separation is somewhat challenging because the compounds all contain a hydrophobic tetrapyrrole core structure, and many differ subtly on the basis of the nature of the appended substituents; for example, tolyporphins A–D and L–O each contain two *C*-glycosides, and tolyporphins G and H each contain one OAc and one OH group, thus presenting quite similar polarities. Mass spectrometric analysis faces the (isobaric) challenge that tolyporphins G,H are isomers, as are tolyporphins L-O. Absorption spectroscopy faces the first challenge that all tolyporphins A–R exhibit absorption bands that overlap with that of chlorophyll *a*, which is abundant in cyanobacteria, and the second challenge that the of the 18 tolyporphins, fourteen (A–J and L–O) are dioxobacteriochlorins, three (K, Q and R) are oxochlorins, and one (P) is a porphyrin. The dioxobacteriochlorins absorb similarly but not identically with each other, and the same phenomenon is observed for the three oxochlorins, presenting the problem of absorption spectral aliasing[20] – the absorption spectrum of such a mixture cannot be unambiguously deconvolved to give the quantities of the individual constituents. Moreover, the

reported absorption spectra differ considerably among tolyporphins for which the chromophore is ostensibly identical, imparting uncertainty in analysis.

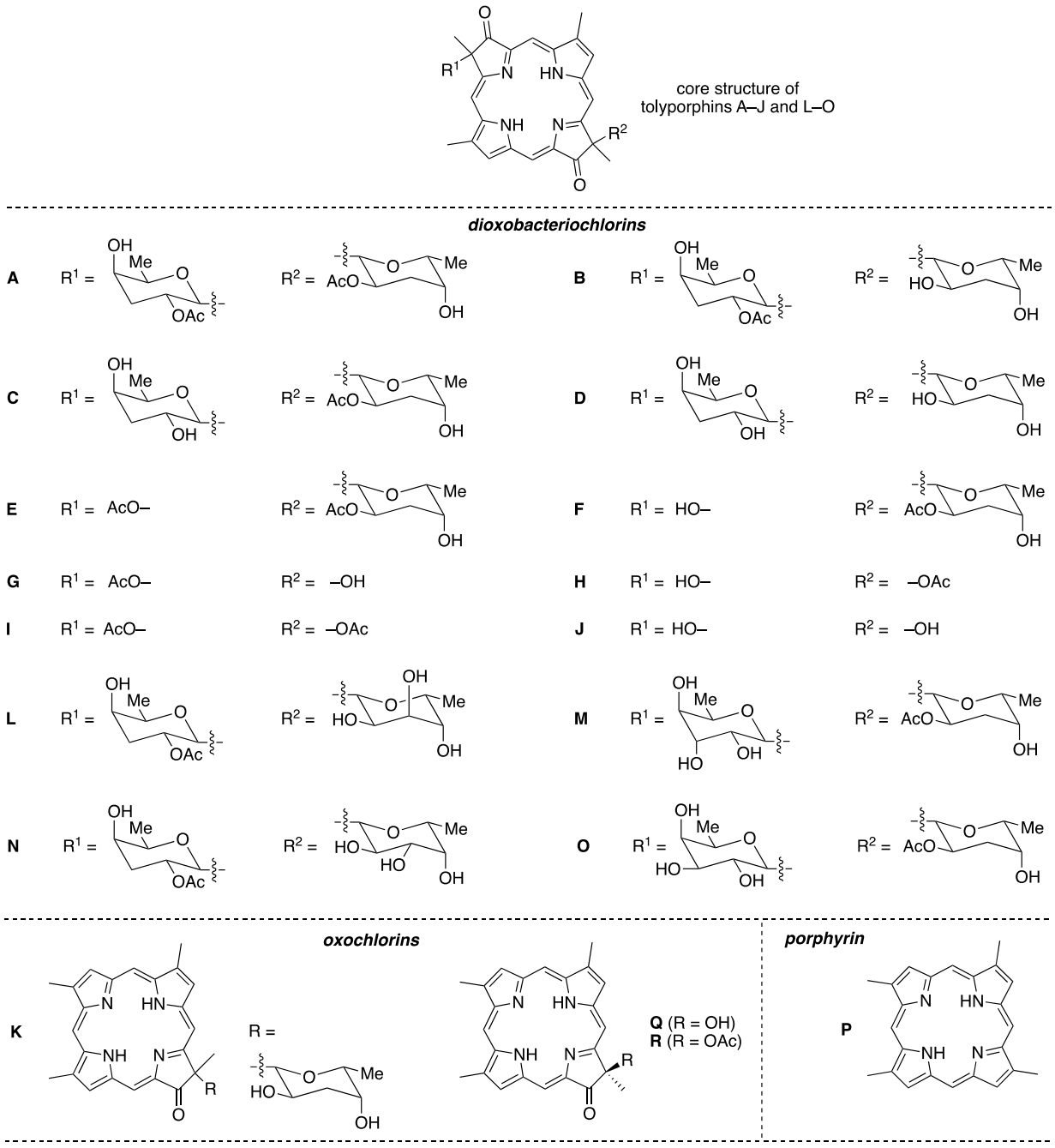

Chart 2. Tolyporphins A–R.

In this paper, we first examine the distributions of members of the tolyporphin family that have been reported over the years from the HT-58-2 culture, the only known producer of

tolyporphins and the culture originally collected at Nan Madol in Pohnpei. We then characterize extracts of the HT-58-2 culture grown under media containing different soluble nitrogen sources (ammonium versus nitrate); the characterization is performed by liquid chromatography mass spectrometry using dynamic multiple reaction monitoring. Multiple tolyporphins are still found to co-elute on chromatography. The yield of tolyporphins remains considerably less than that from the culture reported nearly 30 years ago, but the presence of both ammonium and nitrate salts is found to promote production of tolyporphins. The absorption spectra of all available tolyporphins are presented. The absorption spectra are compared with those of synthetic dioxobacteriochlorin, oxochlorin, and porphyrin analogues, as well as with synthetic analogues of tolyporphin A. Taken together, the work advances analytical capabilities for assessing the various members of this distinctive family of tetrapyrrole natural products.

RESULTS AND DISCUSSION

Isolation of tolyporphins

The isolation of tolyporphins has been reported on five occasions over a 25-year period.[2,5,12-14] In each case, the isolation was from the culture HT-58-2. During this period, additional tolyporphins have been identified as purification methods have become more sophisticated and applied with increasing vigor. Different growth conditions also have been employed, and the extent to which the cyanobacterial strain may have changed is unknown.[5] Indeed, we at the University of Hawaii were able to resurrect the HT-58-2 culture in ~2015 after ~20 years of dormancy. The products obtained upon the five isolations are listed in Table 1.[5,12-14,22] The first column represents data from three publications from Prinsep over a span of several years,[2,12,13] but all those results are most likely from the original cultivation of the HT-58-2 sample. The most recent two isolations (columns 2 and 3) were carried out in the past few years

with the resurrected HT-58-2 culture.[5,14] The final column contains previously unpublished LC-MS analysis of extracts from the HT-58-2 culture grown in two different media conditions (A3M7[1] and BG11[21]), with the relative peak area for each component determined by multiple reaction monitoring (MRM[23,24]). In each case, tolyporphin A is the dominant member among the tolyporphin family.

Table 1. Isolations of tolyporphins.

Component	**Isolations of tolyporphins**					
	Prinsep[12]	Zhang[5]	Gurr[14]	Dai (here)	Gurr,[14] Rel. Abund.	
					A3M7	BG11[f]
Freeze-dried Biomass	93 g	79.5 g	79 g	N/A[d]		
Lipo extract	7.5 g	4.75 g	4.7 g	2.94 g		
A	123 mg (0.1%)	6.2 mg		19 mg	22.0%	11.0%
B, C	38 mg (4:1) (0.032, 0.008%)	3.0 mg		3.0 mg	1.7%	1.6%
D	5 mg (0.005%)	0.8 mg		1.0 mg	0.8%	1.0%
E	46 mg (0.049%)	2.0 mg		7.5 mg	11.4%	2.8%
F	12 mg (0.013%)	0.5 mg		1.0 mg	6.0%	3.9%
G, H	-- mg (2:1) (0.004, 0.002%)	1.0 mg		1.5 mg	1.5%	1.7%
I	1.5 mg (0.002%)	0.5 mg		2.0 mg	13.5%	9.4%
J	1.5 mg (0.0016%)[a]			3.0 mg	0.5%	1.2%
K	1 mg (0.0011%)[a]	0.4 mg		1.0 mg	4.8%	4.7%
L, M	3.5 mg (2:1)[b] (0.0025, 0.0013%)		0.9 mg (0.0011%)[c]	3.5 mg	0.6%[e]	0.9%[e]
N, O			2.3 mg (0.0029%)[c]	0.8 mg		
P			1.0 mg (0.0013%)[c]	1.0 mg	13.1%	20.4%
Q			3.5 mg		5.2%	2.7%

			(0.0044%)[c]			
R			1.0 mg (0.0013%)[c]		18.8%	38.7%

[a]Ref 13. [b]Ref 22. [c]The calculated yield reported here is based on the yield of the lipophilic extract, not freeze-dried algal mass. The values for tolyporphins L,M and N,O reported previously[14] contain typographic errors (0.002% and 0.005% rather than the correct values of 0.02% and 0.05%). To facilitate comparison this is expressed as algal yield here. [d]The exact mass of algae is unknown as only a portion of the algae mass was extracted. [e]Tolyporphins L-O are isobaric and coelute in this LC-MS method, so only the total amount of L-O could be estimated. [f]Relative percentage of total tolyporphins detected by LC-MS (based on MRM peak area normalized to the internal standard) for a 30-day culture in A3M7 and BG-11 media based on three biological replicates.

Inspection of Table 1 reveals the following.

First, exact media conditions play a large role in the overall yield as we have previously reported;[5] as one example, the relative amount of tolyporphin A is twice as much in A3M7 media compared to BG11 (columns 5 and 6). A3M7 and BG-11 media differ in the nature of the soluble nitrogen source; the former contains ammonium salts and sodium nitrate whereas the latter contains only sodium nitrate.

Second, repeated attempts to obtain yields similar to those originally reported by Prinsep and coworkers.[12,13,22] have been largely unsuccessful. There may be multiple reasons for this discrepancy. Subsequent efforts to improve yields through media studies indicate the amount of tolyporphins and cyanobacterial biomass produced are sensitive to the nitrogen source, and often inversely related. The original paper reports cultivation in BG-11 media, but we have shown growth using ammonium chloride produces much higher amounts of tolyporphin A. Unfortunately, the latter conditions essentially kill the culture in around 25 days resulting in production of very little biomass. The net effect with ammonium chloride was lower isolated yields. Interestingly, growth in A3M7 media produced a 10x greater gravimetric yield of tolyporphin A from a vibrant culture. Based on these results, and laboratory records from the 1990s indicating the HT-58-2 culture had been grown in A3M7, we suspect A3M7, or a similar

media, was used instead of the reported BG-11. Even in A3M7, however, our recent yields have failed to match the previously reported production level. In our experience, titers of cultured compounds often decrease with repeated culturing, and so "age" may be another factor. This observed decrease is possibly related to removal of environmental pressures that resulted in the evolutionary origin of tolyporphins, and repeated cryogenic storage.

Third, isolated yields of the tolyporphins are dependent on how long the culture is grown. For example, the overall yield of tolyporphin A is maximized by a growth period of ~40 days.[5] Fourth, the observed distribution of the members of the set of tolyporphins is also dependent on growth time, and there appears to be a general relationship between the extent of *C*-glycosylation/*O*-acetylation and the daily yield of each tolyporphin. For example, analysis by liquid chromatography-mass spectrometry multiple reaction monitoring (LC-MS MRM) suggests that tolyporphins with R^1 and R^2 as OH or OAc groups (tolyporphins G, H and I) have daily production yields that are higher during the first 10 days of growth as measured by relative fold-change of the various derivatives. In contrast, tolyporphins E and F, with one *O*-acetyl-containing *C*-glycoside and one OAc group, have a maximum daily production between days 10-–15, while the daily production of tolyporphin A, with two *O*-acetyl-containing *C*-glycosides, tends to be highest between 20–25 days. The total amount of tolyporphin A accumulated in cells is greatest around day 40, but in our experiments daily production peaks between days 20–25. The significance and driving forces behind the timing of the various derivatives is currently unknown.

The fourth column in Table 4 illustrates the relative amount of each tolyporphin observed in the crude extract when the culture was grown in A3M7 or BG-11 media. These percentages were determined by LC-MS dynamic multiple reaction monitoring (dMRM) analysis[23,24] of three biological replicates which provided an average peak area corresponding to each compound

normalized to the internal standard. While variations in the MS ionization efficiency likely occur that affect the MS response for each dioxobacteriochlorin, oxobacteriochlorin, and porphyrin derivative, the general trends are consistent with the isolated yields. Figure 2 (top panel) shows the annotated dMRM chromatogram of the crude extract of the HT-58-2 culture showing the elution order of the known tolyporphins, while the bottom of Figure 2 shows the same chromatogram based on absorption detection at 400 nm. The latter chromatogram is complicated by coelution of some of the tolyporphins and coelution with other compounds that also absorb at this wavelength. As a result, the absorption spectral and LC-MS-dMRM chromatograms look different. Despite significant efforts, a single chromatographic method to resolve all the components of the mixture remains elusive, hence this dMRM method remains the best way to interrogate the individual components with confidence.

To measure reproducible dMRM chromatographic peak areas within the same batch, an acetonitrile-water mobile phase system modified with ammonium formate was required. Typically, 0.1% formic acid is added to the mobile phase to improve ionization efficiency and peak shape, however under these conditions the observed peak areas of tolyporphin A and derivatives decreased significantly over time in technical replicates, i.e., the same sample measured at the start and end of a sequence yielded vastly different MS peak areas. The immediate concern was that the tolyporphins were degrading during analysis, but peak areas at 400 nm did not show the same degree of variability. A closer inspection of the data revealed that the ratio of the protonated to sodiated ion was changing, leading to the hypothesis that sodium ions, leaching from the glassware, were coordinating with the analytes to yield larger amounts of that adduct over the course of the experiment. After optimization, ammonium formate was selected as an acceptable mobile phase additive. A 1 mM concentration in both H_2O (line A) and 95:5, acetonitrile : H_2O (line B) was sufficient to produce consistent peak areas within a

sequence run. Apparently, NH_4^+ out-competed Na^+ as a proton/charge source, and "suppressed" additional sodiated adduct formation.

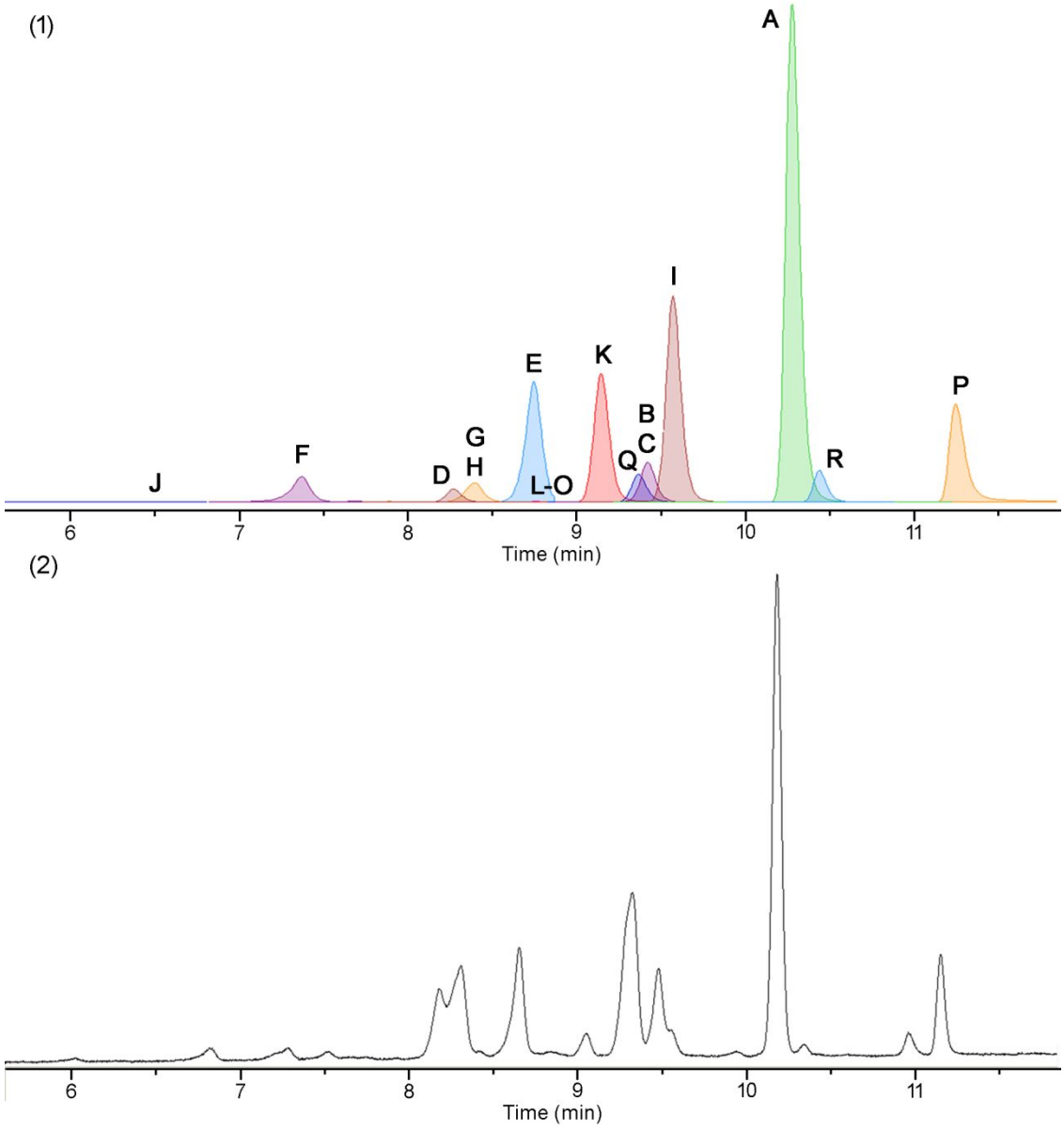

Figure 2. Representative chromatograms of tolyporphins found within the extract of the HT-58-2 culture. Extracted ions for dMRM (1, maximum peak intensity is 3 x 10^4 counts) and extracted absorption at 400 nm (2, maximum peak intensity is 0.34 absorption units).

As added measures of robustness, two semisynthetic tolyporphin derivatives were prepared as internal standards (Chart 3). The acetate groups of the *C*-glycosides of tolyporphins can be easily hydrolyzed in reasonable yield.[25] Thus, tolyporphin A was hydrolyzed to form

tolyporphin D. Both tolyporphins A and D were then treated with butyric anhydride in the presence of triethylamine and 4-(*N,N*-dimethyamino)pyridine to form non-natural standards with properties identical to the tolyporphins. One internal standard, tolyporphin D *O,O,O,O*-tetrabutyrate, was added to the LC-MS sample vials immediately prior to analysis for use as a quantification standard and to account for instrumental drift during analysis. The other semisynthetic derivative, tolyporphin A *O,O*-dibutyrate, was spiked into every harvested cell mass sample at a known concentration prior to extraction and used as a means of assessing extraction efficiency. A vast majority of standard recoveries were within 80 – 120%. For all tolyporphins and derivatives, MRM transitions were selected based on MS/MS fragmentation patterns of the protonated [M + H] parent ion, and optimized for signal intensity over a range of collision energies.

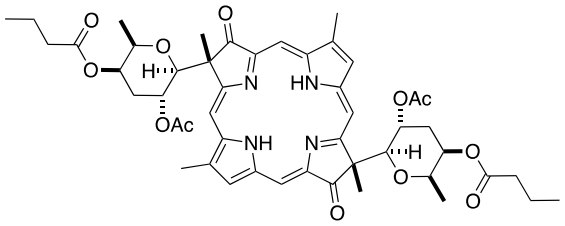

tolyporphin A *O,O*-dibutyrate

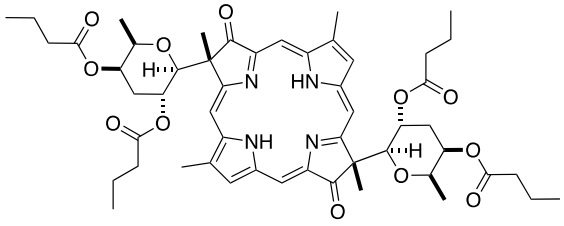

tolyporphin D *O,O,O,O*-tetrabutyrate

Chart 3. Semisynthetic tolyporphin standards.

Absorption spectra

The absorption spectra of tolyporphins A–R are shown in Figure 3. The tabulated spectra are listed in Table 2. Tolyporphins B and C are isomers and are co-isolated, hence the absorption spectrum represents the mixture of the two isomers. Tolyporphins G and H also are co-isolated isomers, for which one absorption spectrum is available. The same situation holds for tolyporphins L and M, and for tolyporphins N and O. Thus, for the 18 known tolyporphins, there are 14 absorption spectra in hand.

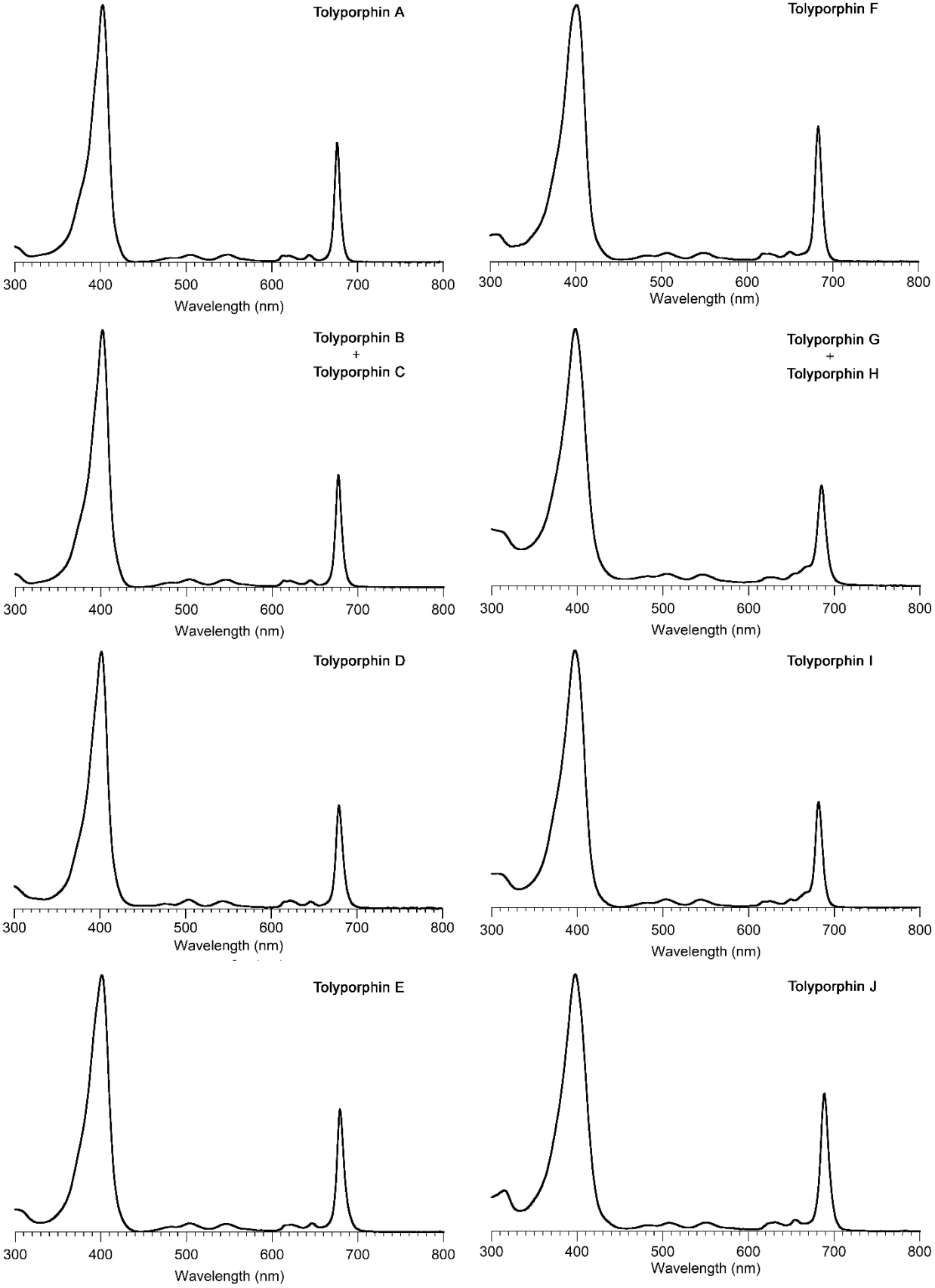
Tolyporphin A
Tolyporphin F
Tolyporphin B
+
Tolyporphin C
Tolyporphin G
+
Tolyporphin H
Tolyporphin D
Tolyporphin I
Tolyporphin E
Tolyporphin J
300
400
500
600
700
800
Wavelength (nm)

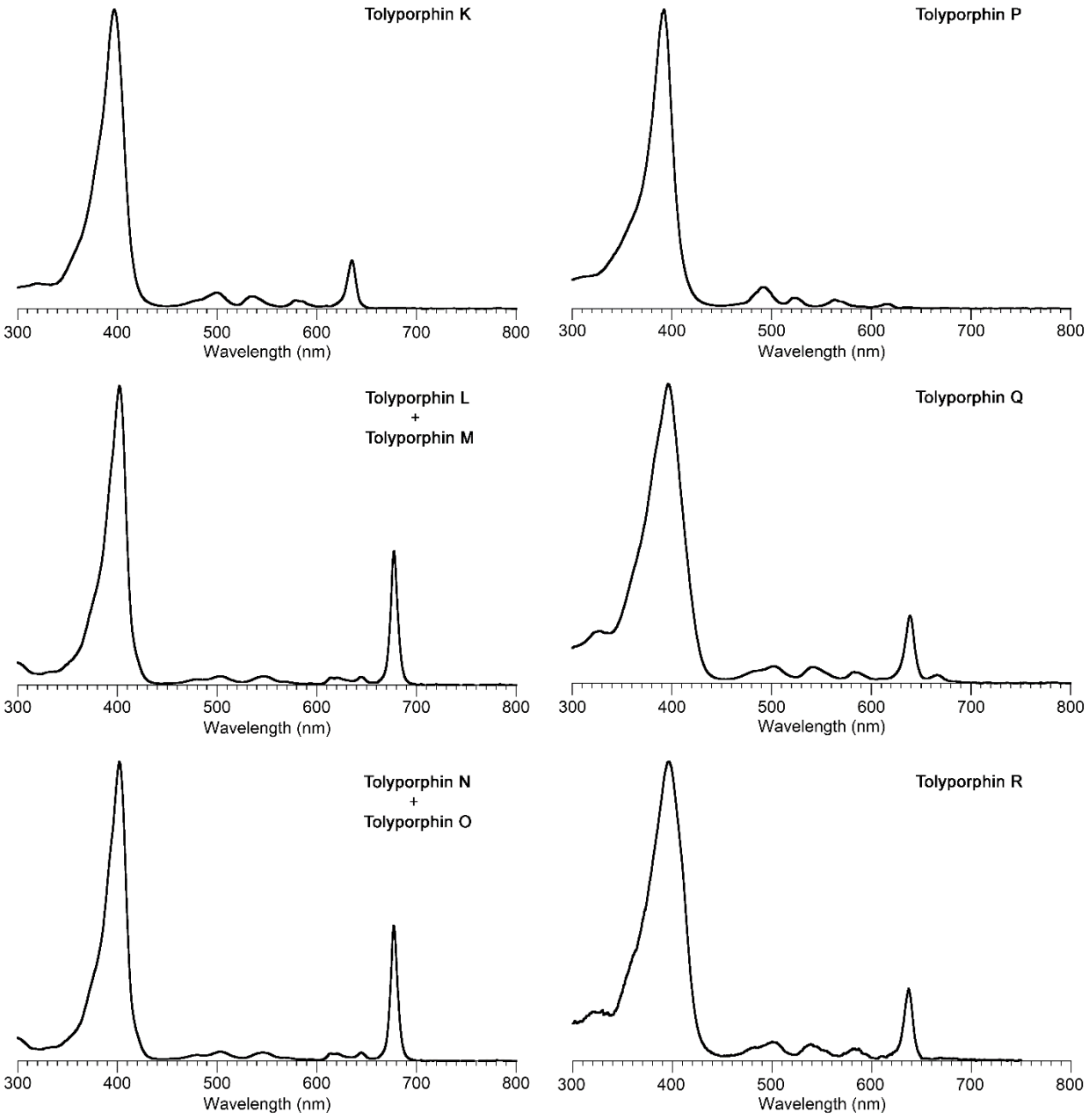

Figure 3. Absorption spectra of tolyporphins in methanol at room temperature.

Table 2. Absorption spectral data of tolyporphins (in methanol).

Tolyporphin	Absorption in nm (fwhm)		I_B/I_Q
	B band	Q_y band	
dioxobacteriochlorins			

A	403 (22.1)	676 (7.6)	2.15
B+C	402 (22.1)	677 (8.4)	2.30
D	402 (23.1)	679 (9.4)	2.48
E	401 (26.7)	679 (9.4)	2.09
F	401 (29.9)	683 (9.3)	1.90
G+H	398 (32.5)	685 (11.5)	2.55
I	397 (30.2)	682 (9.6)	2.44
J	398 (32.2)	689 (10.7)	1.87
L+M	402 (22.3)	678 (8.0)	2.24
N+O	402 (22.3)	677 (8.0)	2.21
oxochlorins			
K	397 (28.7)	635 (10.1)	6.17
Q	396 (42.3)	639 (11.0)	4.42
R	396 (41.6)	637 (10.5)	4.08
porphyrin			
P	392 (26.8)	492 (23.1)	13.9

Molar absorption coefficients

A key issue concerns the molar absorption coefficient (ε) values for the tolyporphins. Values of ε have been reported over the years as individual tolyporphins have been isolated. The reported values are listed in Table 3.[2,11-14,26,27] Values are listed for the B band (also known as the Soret band), the Q_y band, the ratio of the intensities of the B and Q_y bands, and the fwhm of the Q_y band.

Table 3. Absorption spectral data for tolyporphins reported in the literature.

Tolyporphin	Solvent	Absorption in nm (ε in $M^{-1}cm^{-1}$)		I_B/I_Q	fwhm (Q_y), nm	Reference
		B band	Q_y band			
dioxobacteriochlorins						
A	MeOH	401 (49,000)	675 (22,000)	2.23	7.7	Prinsep, 1992[2]

A	EtOH	402 (148,000)	676 (68,500)	2.16	--	Morlière, 1998[11]
A-Ac_2	CH_2Cl_2	406 (107,463)	678 (44,600)	2.41	8.9[e]	Wang, 1999[26]
dia-A-Ac_2[a]	CH_2Cl_2	407 (110,500)	684 (51,530)	2.14	10.8	Minehan, 1998[27]
B, C	MeOH	406 (2,100)[b]	680 (13,000)	0.162[d]	9.0	Prinsep, 1995[12]
D	MeOH	368 (24,000)	680 (12,000)	2.0	8.9	Prinsep, 1995[12]
E	MeOH	388 (16,000)	686 (7,300)	2.19	9.4	Prinsep, 1995[12]
F	MeOH	386 (39,000)	684 (22,000)	1.77	15.3	Prinsep, 1995[12]
G, H	MeOH	368 (18,000)	686 (10,000)	1.80	11.2	Prinsep, 1995[12]
I	MeOH	376 (14,000)	684 (7,800)	1.79	9.6	Prinsep, 1995[12]
J	MeOH	396 (7,900)	688 (1,500)	5.27[d]	--	Prinsep, 1998[13]
L, M	MeOH	401 (130,000)	677 (50,000)	2.5	--	Gurr, 2020[14]
N, O	MeOH	401 (130,000)	677 (50,000)	2.5	--	Gurr, 2020[14]
oxochlorins						
K	MeOH	397 (3,500)	635[c] (380)	9.21	10.6	Prinsep, 1998[13]
Q	MeOH	394 (63,000)	666 (5,000)	12.6	--	Gurr, 2020[14]
R	MeOH	395 (50,000)	636 (13,000)	4.0	--	Gurr, 2020[14]
porphyrin						
P	$CHCl_3$	398 (79,000)	619 (1,300)	--	--	Gurr, 2020[14]

[a]A diastereomer (and *O,O*-diacetate) of the natural compound. [b]A likely typographic error (see text). [c]Other longer wavelength bands with weaker intensity are present. [d]Likely indicates an erroneous ε value or incorrect compound. [e]From the notebook of Dr. W. Wang as provided by Prof. Y. Kishi.[26]

The values vary considerably: for the dioxobacteriochlorins (tolyporphins A–J, L–O), ε ranges from 2,100 – 148,000 $M^{-1}cm^{-1}$ for the B band, and from 1,500 – 68,600 $M^{-1}cm^{-1}$ for the Q_y band. The data were obtained in methanol except for one case where ethanol was employed, which also gave the highest values.[11] It is common that the values for ε vary enormously even for common standards in widespread use. Indeed, the reported value of ε for the B band of *meso*-tetraphenylporphyrin ranges from $<10^5$ to $>10^6$ $M^{-1}cm^{-1}$.[28] At the same time, it is unlikely for the absorption spectra (wavelength positions and integrated absorption) to vary due to small

structural differences of non-conjugated groups appended to the periphery of the macrocycle. Thus, within a given class of tolyporphins – one expects the dioxobacteriochlorins to exhibit similar spectra with one another, and the oxochlorins to exhibit similar spectra to each other. The scientific basis for this expectation originates with the similar molecular orbital energy levels and oscillator strengths exhibited by similar chromophores.

One wrinkle concerning the comparison of tetrapyrrole absorption spectra is that there are two transitions, B_x and B_y, that together give rise to the observed B band. When the two transitions are split apart, the molar absorption coefficient for either band is lower than that when the two transitions coalesce. The integrated band intensity may be quite similar, but the molar absorption coefficient measures the height of a peak, not the integrated band area. In contrast, the Q_y band stems from a single transition. Thus, while the molar absorption coefficient of the B band may vary due to structural perturbation that causes slight shifts in the positions of the B_x and B_y transitions, the molar absorption coefficient of the Q_y band is expected to be more constant.

The ratio of absorbance values of various peaks in the spectrum of hydroporphyrins is a parameter of longstanding use in the tetrapyrrole field to gauge purity for compounds isolated from natural sources.[29] The ratio of the absorbance values at the B band versus the Q_y band (I_B/I_Q) provides a particularly valuable point of comparison.[30] The comparison holds as well for ε values of the respective peaks. While perhaps used more widely in the classical era (e.g., 1950s) predating more modern methods of analysis, the ratio retains value. In short, the (I_{Soret}/I_Q) ratio is expected to be relatively constant across molecules that contain the same π-system and similar substituents attached thereto. With this perspective as backdrop, we now turn to consider the molar absorption coefficient values of synthetic analogues of the various members of the tolyporphin family.

Benchmark synthetic tetrapyrroles

The classes of tolyporphins include dioxobacteriochlorins, oxochlorins, and a porphyrin. Representative synthetic analogues are shown in Chart 4. The analogues include four dioxobacteriochlorins (**diOxo** series), one oxochlorin (**Oxo-OEC**), and two porphyrins (**OEP**, **P**). The two porphyrins differ in the number of β-pyrrole substituents: **OEP** has eight ethyl groups whereas porphine (**P**) has none. Because **Oxo-OEC** has a full complement of β-pyrrole substituents, and we sought to understand the effects (if any) of the β-alkyl substituents versus the chromophore alone, two unsubstituted chlorins (**C**, **C-Me**) were included. The reported spectral parameters of selected porphyrins, chlorins, oxochlorins, and dioxobacteriochlorins are listed in Table 4.[31-48]

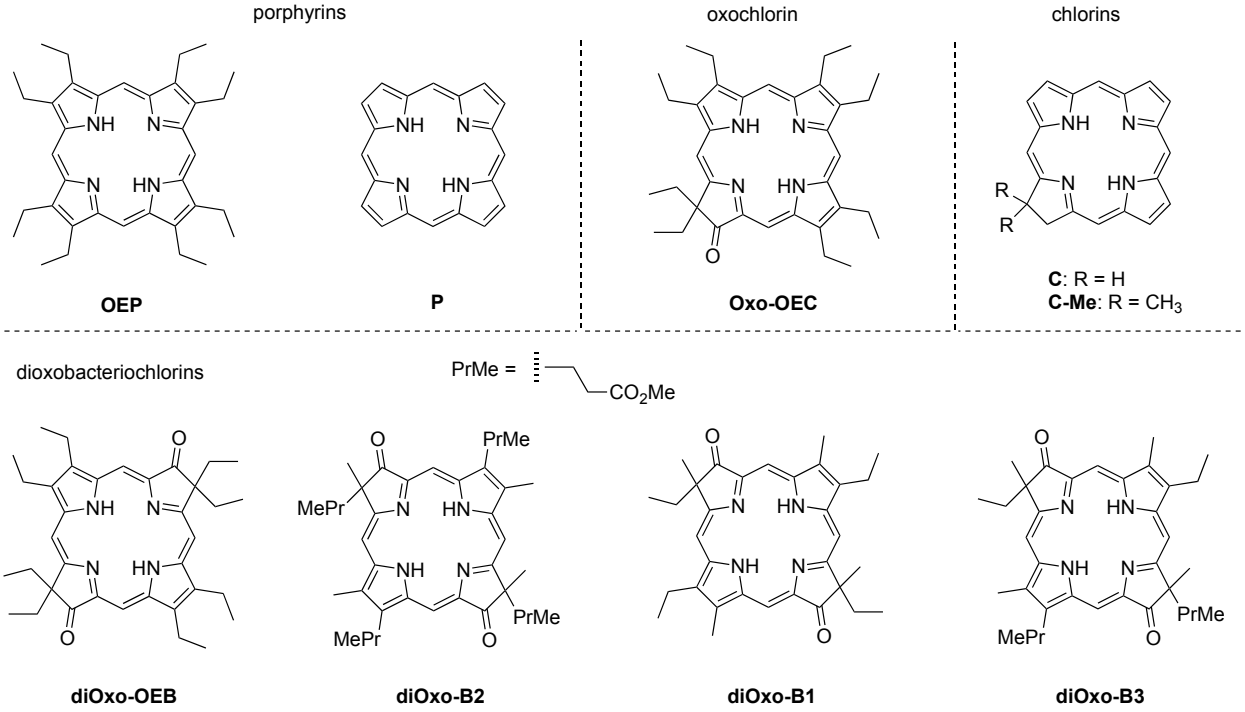

Chart 4. Synthetic tetrapyrrole macrocycles.

Table 4. Absorption spectral data for synthetic tetrapyrrole macrocycles.

entry	compound	solvent	B band	Q band[a]	I_B/I_Q	fwhm (B) nm	fwhm (Q) nm	Ref
porphyrins								
1	**P**	benzene	395 (261,000)	490 (15,000)	17.4	17[b]	21.2[b]	31
2	**P**	benzene	396 (234,000)	489 (14,100)	16.6	17	20	32
3	**P**	CH_2Cl_2	394 (272,000)	489 (16,400)	16.6	17	21	33
4	**OEP**	benzene	400 (159,000)	498 (14,500)	11.0	35[b]	24.4[b]	34
5	**OEP**	$CHCl_3$	401 (167,000)	499 (13,300)	12.6			35
6	**OEP**	$CHCl_3$	399 (178,000)	498 (13,500)	13.2			36
chlorins and oxochlorins								
7	**Oxo-OEC**	benzene	401 (108,000)	644 (34,000)	3.18			37
8	**Oxo-OEC**	$CHCl_3$	- -	642 (32,900)	- -			38
9	**Oxo-OEC**	$CHCl_3$	408 (151,000)	642 (30,400)	5.0	32	12	39
10	**Oxo-OEC**	CH_2Cl_2	403 (186,000)	640 (38,800)	4.80	31.4	12.5	40
11	**Oxo-OEC**	CH_2Cl_2	406 (198,000)	640 (40,600)	4.88			41
12	**C**	benzene	388 (128,000)	638 (50,000)	2.56			42
13	**C**	benzene	389 (126,000)	638 (50,700)	2.49	35.3	10	32
14	**C-Me**	toluene	389 (158,000)	634 (66,100)	2.39	32.7	9.2	43
15	***trans*-OEC**	benzene	392 (183,000)	646 (68,600)	2.67			34
16	***trans*-OEC**	benzene	392 (187,000)	647 (75,200)	2.49			32
17	***trans*-OEC**	$CHCl_3$	392 (155,000)	644 (48,500)	3.20			35
dioxobacteriochlorins								
18	**diOxo-OEB**	$CHCl_3$	402 (165,000) 413 (192,000)	691 (96,300)	1.99			44
19	**diOxo-OEB**	CH_2Cl_2	407 (117,000)	691 (52,000)	2.09	24.7	11.1	40

20	**diOxo-B1**	CH_2Cl_2	398 (171,000) 409 (191,000)	687 (110,000)	1.74			45
21	**diOxo-B1**	CH_2Cl_2	400 (179,000) 408 (198,000)	684 (104,000)	1.90			46
22	**diOxo-B2**	CH_2Cl_2	401 (164,000) 411 (187,000)	685 (95,000)	1.97			47
23	**diOxo-B3**	CH_2Cl_2	408 (189,000)	684 (90,000)	2.10			46

[a]Each band refers to the most intense spectral feature in the visible region: the Q(1,0) band for porphyrins, the Q(0,0) band (i.e., Q_y) for chlorins and oxochlorins, and the Q(0,0) band (i.e., Q_y) for dioxobacteriochlorins. [b]The spectral trace was taken from PhotochemCAD.[48]

The following observations are germane to the case of tolyporphins.

(1) The intensity and fwhm of the B band of the unsubstituted porphyrin (**P**) and octaethylporphyrin (**OEP**) are counterbalanced: the B band for **P** is sharp whereas that for **OEP** is somewhat broader. Thus, the absorption coefficient of **P** is ~1.5 times larger than that of **OEP**, which is compensated by ~2 times larger fwhm (from 17 to 35 nm) of the B band of **OEP** compared to **P**. On the other hand, the absorption coefficients and fwhm of the Q(1,0) band of **P** and **OEP** are almost constant regardless of the number of substituents, which are ~14,500 $M^{-1}cm^{-1}$ and ~22 nm, respectively (Table 4, entries 1–6). The Q(1,0) band of a free base porphyrin is typically the most intense absorption band in the visible region. Thus, the molar absorption coefficients of porphyrin tolyporphin P, bearing four meso-methyl substituents, can be estimated based on the molar absorption coefficient of the Q(1,0) band: 14,500 $M^{-1}cm^{-1}$ for the Q(1,0) band (492 nm) gives 200,000 $M^{-1}cm^{-1}$ for the B band at 392 nm.

(2) There are five reports on the molar absorption coefficients of octaethyloxochlorin (**Oxo-OEC**) as shown in Table 4 (entries 7–11). The ε values for the Q_y band are quite similar across the five reports, with average of ~35,000 $M^{-1}cm^{-1}$. The comparison between unsubstituted chlorins **C** and **C-Me** (entries 12–14) versus octaethylchlorin (***trans*-OEC**, entries 15–17) shows that the number of alkyl substituents at the meso-positions of chlorins has an insignificant effect on the Q_y molar absorption coefficient. The molar absorption coefficient of the oxochlorin lacking β-pyrrole substituents is not known, but we assume that a similar trend holds for oxochlorins. Thus, a value of 35,000 $M^{-1}cm^{-1}$ is expected for the Q_y band of oxochlorins.

(3) There are six relevant reports concerning the dioxobacteriochlorins **diOxo-OEB**, **diOxo-B1**, **diOxo-B2**, and **diOxo-B3** (Table 4, entries 18–23). Oxidation was carried out at relatively large scale of octaethylporphyrin, etioporphyrin II, coproporphyrin II tetramethyl ester, or mesoporphyrin IX dimethyl ester to afford the corresponding **diOxo-B1** (74 mg),[45] **diOxo-B1**

(75 mg[46]), **diOxo-B2** (9.5 mg),[47] or **diOxo-B3** (77 mg).[46] Although the quantity of the dioxobacteriochlorin employed for measurement of the molar absorption coefficient was not reported, the resulting values are likely less error-prone than when only small quantities of samples are available. In five of the six reports, the ε value of the B band was similar across the compounds, and the ε value of the Q_y band was similar across the compounds. On this basis, the value of ε for the Q_y band of synthetic dioxobacteriochlorins is taken to be 100,000 $M^{-1}cm^{-1}$.

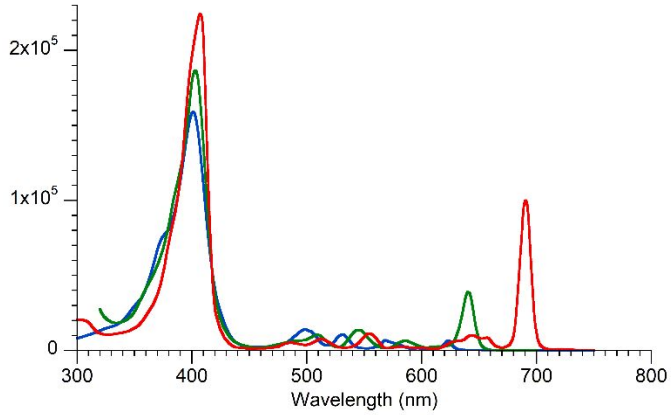

Figure 4. Absorption spectra of reference synthetic tetrapyrroles. Octaethylporphyrin (**OEP**, blue), octaethyloxochlorin (**Oxo-OEC**, green), and dioxobacteriochlorins **diOxo-OEB**, red).

Synthetic tolyporphin derivatives

A further spectral comparison is provided by the synthetic analogues of tolyporphin A, which were used to establish the molecular structure of the native macrocycle. The synthesis of tolyporphin A *O,O*-diacetate (Figure 5), a diacetate derivative of tolyporphin A, was carried out in pioneering work by Minehan, Wang and Kishi.[25,26] The first synthesis yielded the reported *O,O*-diacetate of tolyporphin A,[25] but this was found to be a diastereomer of the natural macrocycle.[49] A subsequent synthesis gave the *O,O*-diacetate of the correct stereoisomer of tolyporphin A (the additional acetate groups are shown in magenta in Figure 5).[26] More recent

structural confirmation has come from the single-crystal X-ray structural analysis of tolyporphin A, which shows the projection of the two glycoside moieties on one face of the tetrapyrrole macrocycle. The absorption spectra of tolyporphin A *O,O*-diacetate diastereomer (**dia-A-Ac$_2$**) and tolyporphin A *O,O*-diacetate (**A-Ac$_2$**) are shown in Figure 5. The spectra closely resemble those of the native tolyporphins, congruent with the expected insignificant effect of an acetate group positioned some distance from the dioxobacteriochlorin chromophore.

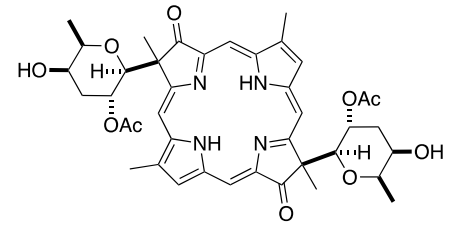

dia-A-Ac$_2$
diastereomer of tolyporphin A *O,O*-diacetate

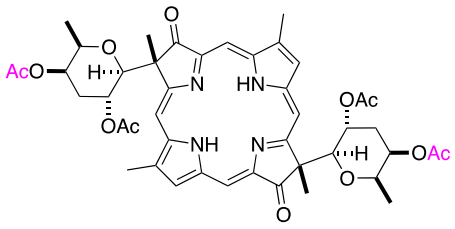

A-Ac$_2$
tolyporphin A *O,O*-diacetate

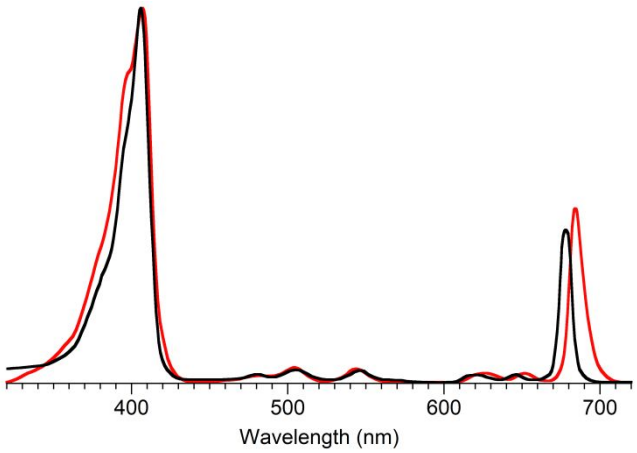

Figure 5. Absorption spectra (normalized) in CH_2Cl_2 of tolyporphin A *O,O*-diacetate diastereomer (**dia-A-Ac$_2$**, red line)[27] and tolyporphin A *O,O*-diacetate[26] (**A-Ac$_2$**, black line).

Composite absorption spectra of multiple pigments

The cyanobacterial culture HT-58-2 produces a family of tolyporphins. Two challenges arise in quantitation of the culture or in bioprospecting for other producing cultures: (1) the composition of the various tolyporphins is not known *a priori*, and (2) the spectra of the various tolyporphins are not identical. The spectra of the various classes (dioxobacteriochlorin, oxochlorin, porphyrin) are distinct, yet the individual members within the dioxobacteriochlorin class or the oxochlorin class (there is only one porphyrin to date) of the tolyporphin family do not exhibit identical peak maxima with each other, although the spectra shapes are nearly superposable. This issue is highlighted by the overlays provided in Figure 6.

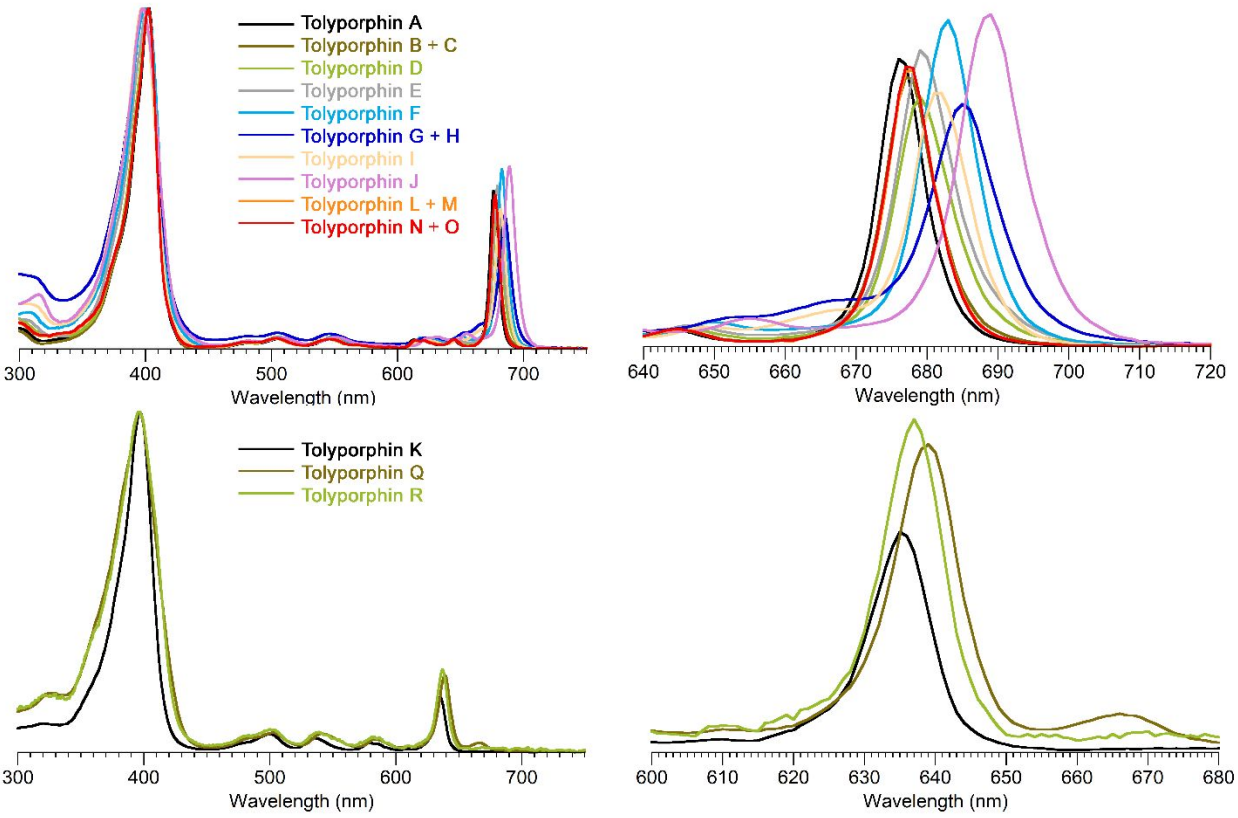

Figure 6. Overlay of spectra of members of a given class of tolyporphins. Dioxobacteriochlorin tolyporphins (upper left) with spectral expansion (upper right). Oxochlorin tolyporphins (lower left) with spectral expansion (lower right).

The challenge of "aliasing" – where a composite spectrum is under-determined because of overlapping yet insufficiently distinct spectra of the components – is known.[20] Thus, deconvolution of a spectrum of a mixture of tolyporphins cannot be reliably carried out to determine the composition even though the individual spectra are known. On the other hand, one can work forward to generate representative composite spectra for various mixtures of tolyporphins. Indeed, with the individual absorption spectra and molar absorption coefficients in hand, composite spectra can be generated at will. Here we show several composite spectra. In one case, each tolyporphin is present in equal molar amounts. In a second case, tolyporphin A comprises 50%, the remaining dioxobacteriochlorin tolyporphins collectively constitute 40% (equal amounts for each), and the remaining tolyporphins comprise 10% (again, equal amounts for each). In each case, the aforementioned standard molar absorption coefficient values have been employed. These include: ε for the Q band of tolyporphins A–J and L–O is 100,000 $M^{-1}cm^{-1}$; ε for the major Q band of tolyporphins K, Q and R is 35,000 $M^{-1}cm^{-1}$; and ε for the Q(1,0) band of tolyporphin P is 14,500 $M^{-1}cm^{-1}$. The composite spectra are shown in Figure 7. Note that any errors in assessing values of the respective molar absorption coefficient, if applied systematically across all compounds, would afford the same ratios of components.

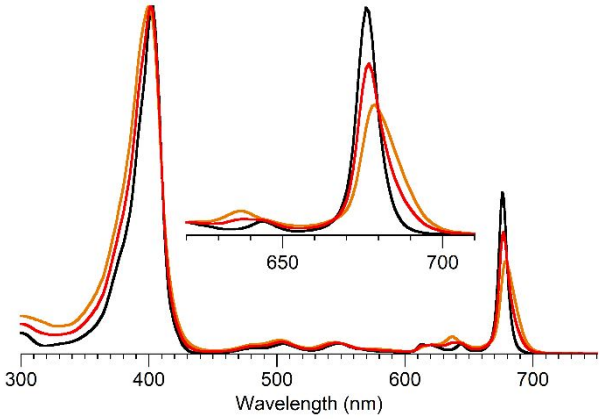

Figure 7. Composite spectra of tolyporphins. Tolyporphin A (black), tolyporphins A–R in equal ratio (orange), and tolyporphin A = 50% with the sum of B–R = 50% (red).

Availability of spectra

A long-term objective to collect absorption spectra of diverse compounds and make such spectra widely available gave rise to the PhotochemCAD initiative. PhotochemCAD consists of a program of calculational modules for the photosciences[50] and accompanying digital databases of absorption and fluorescence data (300 common organic compounds,[48] 150 members of the chlorophyll family[51]). The databases include the molar absorption coefficient (ε, in $M^{-1}\cdot cm^{-1}$) and the fluorescence quantum yield (Φ_f), where available, information pertaining to solvent, and citations to the originating literature. Accumulating such databases remains a challenge.[52,53] The PhotochemCAD program, prior databases, and the digital absorption spectral data for the tolyporphins described herein are provided for free downloading at www.photochemcad.com. The tolyporphins absorption spectra here include the fourteen available for tolyporphins A–R, tolyporphin A *O,O*-diacetate, and tolyporphin A *O,O*-diacetate diastereomer.

OUTLOOK

The tolyporphins challenge our understanding of the roles of tetrapyrroles in nature, as almost all tetrapyrroles function as enzymatic cofactors, not as a collection of natural products. Deciphering and quantitating the distribution of tolyporphins appears (beguilingly) simple but the presence of structures of similar polarity complicates chromatography, the isobaric members present limitations to mass spectrometry, and the similar but non-identical absorption of subsets of tolyporphins limits use of absorption spectroscopy. The studies reported herein provide a comprehensive treatment of tolyporphins A–R, which have been described previously in disparate reports. The finding that ammonium and nitrate salts together promote production of tolyporphins, albeit not in the quantity first reported 30 years ago, is intriguing and compels additional studies of other conditions. The methods employed here should provide the foundation for numerous studies and exacting studies of these most unusual tetrapyrrole macrocycles.

EXPERIMENTAL

Isolation and purification of tolyporphins

The HT-58-2 strain was grown in A3M7 media in Pyrex carboys (volume up to 20L) with aeration at a flow rate of 5 L/min and in continuous fluorescent illumination. Cell material was harvested after 45 days of growth by decantation and filtration. The cell mass was then freeze-dried, exhaustively extracted in 1:1 dichloromethane : 2-propanol, dried in vacuo and stored at –20° C. The crude extract was subjected to a modified Kupchan partition[54,55] into hexanes, dichloromethane, and aqueous methanol soluble fractions. The hexanes and dichloromethane extracts were then separately subjected to C8 solid-phase extraction and eluted with an H_2O : MeOH (0.1% formic acid) gradient of 25%, 50%, 75%, 90% and 100%. The 75%

MeOH fraction of the dichloromethane partition and the 90% MeOH fraction of the hexanes partition were then further purified by reverse-phase chromatography followed by normal phase chromatography. From several previous extractions of the HT-58-2 strain, cultured and partitioned as stated above, various pooled vials of putative tolyporphin compounds were collected, dried and stored at –20 °C for later analysis. From these collections, HRMS data was used to guide selection of mixes that could lead to the desired tolyporphins.

Tolyporphin F was isolated and purified from its mixture on a Phenomenex Luna 5µ PFP (2) 100Å semi-prep column (250 x 10 mm) using A: H_2O (0.1% formic acid); B: acetonitrile (0.1% formic acid) with an 82% B isocratic method, photodiode array detection and a flow rate of 2.5 mL/min (t_R = 12.2–12.6 min). This was followed by normal phase chromatography using a Phenomenex Luna 10µ Silica (2) 100 Å semi-prep column (250 x 10 mm) using A: hexane; B: ethyl acetate with a gradient of 20%–75% B from 1–30 min; 75-100% B 30–40 min; 100% B 40–50 min, detection at 400 nm and flow rate of 3.0 mL/min at retention time of 28.5–31 min.

Tolyporphin J (t_R = 17.0–18.8 min) was isolated from its mixture by the reverse-phase conditions shown for tolyporphin F but instead using a 70% B isocratic method. Tolyporphin J did not require normal phase for further purification.

For tolyporphin K (t_R = 28.7–30.2 min), isolation from three pooled mixtures were required to acquire enough material to confirm the structure by ^{1}H NMR spectroscopy using the reverse-phase conditions of a Phenomenex Luna 5µ C18 (2) 100 Å semi-prep column (250 x 10 mm) using A: H_2O (0.1% formic acid); B: MeOH (0.1% formic acid) with an 85% B isocratic method, photodiode array detection and flow rate of 2.8 mL/min. This was followed by normal phase chromatography using the same conditions as tolyporphin F (t_R = 29.0–32.0 min)

Scant amounts of tolyporphin Q were evident by HRMS and isolated from several mixtures before ultimately being pooled to confirm the structure by ^{1}H NMR spectroscopy prior

to normal phase purification with conditions as for tolyporphin F (t_R = 14.6–16 min). As an example of reverse-phase conditions for one mixture, tolyporphin Q was isolated with same conditions shown for tolyporphin F (t_R = 19.5–21.0 min).

Tolyporphin R was isolated from a mixture using the reverse-phase conditions shown for tolyporphin K but instead using an 86% B isocratic method and flow rate of 2.7 mL/min (t_R = 25.0–26.5 min). The same normal phase conditions as the previous tolyporphins were utilized for further purification with a final retention time of 12.5–13.5 min.

Tolyporphins standards

Tolyporphin D *O,O,O,O*-tetrabutyrate. HRMS ESI: measured *m/z* 939.4743 $C_{52}H_{66}N_4O_{12}$ (-0.7 ppm).

Tolyporphin A *O,O*-dibutyrate. HRMS ESI: measured *m/z* 905.3907 $C_{48}H_{58}N_4O_{12}$ Na^+ (-4.6 ppm).

LC-QqQ-MS/MS analysis of tolyporphins

The freeze-dried algal biomass (2–15 mg in an 8 mL borosilicate glass vial) was treated with dichloromethane–isopropyl alcohol (4 mL, 1:1) and an ethanolic solution of tolyporphin D *O,O,O,O*-tetrabutyrate (200 ng). The biomass was vortexed, sonicated and shook overnight, then the solvent was decanted, and the residual biomass extracted two more times with DCM:iPrOH. The combined solvent extracts were concentrated using an EZ-2 centrifugal evaporator. The crude residue from each sample was re-suspended via sonication in 1 mL of LC-MS-grade 95:5, acetonitrile : H_2O containing 1 mM ammonium formate (diluent) and passed through a 0.45 μm PVDF filter disk into a clean vial. The filtered extract was transferred to a 1.5 mL borosilicate LC-MS sample vial and diluted as necessary to a vial volume of 0.5 mL. Prior to analysis, 50 μL

of a 5.5 μg/mL tolyporphin A *O,O*-dibutyrate solution was added to each sample vial as the quantification standard.

Quantitative analysis of the tolyporphins was conducted on an Agilent 6410 QqQ LC-MS system with electrospray ionization operating in the positive mode. Chromatographic separations were performed on a Kinetex 2.6 μm, 100 x 4.6 mm, 100 Å, C8 UPLC column from Phenomenex. Solvent was delivered by an Agilent 1200 HPLC system with single wavelength detection at 400 nm. Method conditions consisted of an initial hold for 1 min at 40% B (A: H_2O with 1 mM ammonium formate, B: 95:5, acetonitrile : H_2O with 1 mM ammonium formate), followed by a linear gradient to 100% B over 9 min and then held for 5 min. The flow rate was 0.8 mL/min. Quantitative ions for each compound were selected based on the most prominent transition peak detected from product ion MS/MS scans. The collision energy of the parent ion for each transition was optimized over a range of 10 – 50 eV with a step of 5 eV. Retention times for each tolyporphin transition ion peak were noted and programmed for detection by dynamic multiple reaction monitoring (dMRM), which is a time directed method designed to automatically optimize analysis dwell time based on the number overlapping transitions (Table 5). Stock solutions of tolyporphin A, tolyporphin A *O,O*-dibutyrate, and tolyporphin D *O,O,O,O*-tetrabutyrate were prepared in absolute ethanol in concentrations of approximately 5 μg/mL. The exact concentration of these authentic standards was determined using their absorption at 402 and 676 nm assuming the previously reported molar absorption coefficients of 148,000 and 68,500 $M^{-1}cm^{-1}$ for tolyporphin A, respectively.[11] Subsequent work in the present paper indicates a molar absorption coefficient for tolyporphin A of 100,000 $M^{-1}cm^{-1}$ (402 nm) would be more appropriate. While this change affects the absolute concentration of each tolyporphin determine by LC-MS (as the slope of the calibration curve is modified), the relative percent composition values reported in Table 1 are unchanged. A mixed standard calibration

curve of tolyporphin A and the synthetic tolyporphin D *O,O,O,O*-tetrabutyrate was prepared through serial dilution in LC-MS vials in a concentration range from 1000 – 6.25 ng/mL. To each standard, 50 uL of 5.5 μg/mL of the tolyporphin A *O,O*-dibutyrate was added.

Table 5. dMRM data for tolyporphins

Compound	Precursor Ion	Product Ion	Collision Energy (eV)	Ret Time (min)
Tolyporphin A	743	571	20	10.23
Tolyporphin B-C	701	571	20	9.39
Tolyporphin D	659	529	20	8.24
Tolyporphin E	629	397	35	8.37
Tolyporphin F	587	415	20	7.33
Tolyporphins G,H	473	385	30	8.37
Tolyporphin I	515	455	10	9.52
Tolyporphin J	431	413	15	2.51
Tolyporphin K	513	383	30	9.1
Tolyporphins L-O	717	571	25	8.73
Tolyporphin Q	399	384	30	9.32
Tolyporphin R	441	353	35	10.39
Tolyporphin P	367	352	35	11.19
$(Butyryl)_2$-Toly A	883	641	25	12.6
$(Butyryl)_4$-Toly D	939	669	25	13.62

Spectral handling

The absorption spectra of tolyporphins were recorded over a period of two decades using various absorption spectrometers. Each instrument has a distinct setup for outputting spectral data with respect to the wavelength intervals: some instruments output spectral data in integer (e.g., 1 or 2 nm) intervals or in intervals of constant decimal units (e.g., 0.2 or 0.5 nm). To compare and utilize these variegated data, unification of the interval increments is required.

When the data intervals are in equal increments, such data can be aligned by skipping every x entries using spreadsheet software; for example, the 0.2 nm interval data can be converted into 1 nm interval data by picking 1 entry out of every 5 entries.

The situation becomes far more complicated when wavelength intervals of wavelength are available only in random intervals. Two scenarios prevail: (i) Some absorption spectrometers only provide spectral data in random increments in wavelength (close to 1 nm intervals, but not exactly, e.g., 0.97, 0.92, 1.11, 0.95, etc.), and (ii) digitization from published articles and literature typically results in random increments.[51]

The PhotochemCAD 3 program provides a venue for wavelength interpolation in 1-nm intervals with the "Spectrum math" function. By summing a source spectral trace that is in random intervals (spectrum A) and zero-filled dummy data (y-axis data are zero across the entire wavelength region, spectrum B), a resulting spectrum (C) is obtained 1-nm intervals. An example database for doing so is provided at the PhotochemCAD website. The process entails a facile linear interpolation between datapoints of the source spectrum. Some commercial software might also include more sophisticated (bilinear, polynomial, spline) interpolations, which would provide smooth and accurate spectral trace.

For the spectra presented herein, all fourteen absorption spectra (for tolyporphins A–R) were available as XY-datafiles from absorption spectrometers, albeit with absorption intensity in non-uniform and non-integer intervals. Such data were converted using the PhotochemCAD 3 program into 1-nm data intervals. The resulting spectra are displayed in Figures 3 and 6. The spectral data in Figure 4 (synthetic porphyrin, oxochlorins, and dioxobacteriochlorins) and Figure 5 (synthetic tolyporphin A analogues **dia-A-Ac$_2$** and **A-Ac$_2$**) were digitized from print spectra, which affords XY-datafiles with absorption intensity in non-uniform and non-integer intervals. Such data were converted using the PhotochemCAD 3 program into 1-nm data

intervals. The generation of spectral data in uniform intervals is essential for the generation of composite spectra as shown in Figure 7.

Conflict of Interest: There are no conflicts of interest to declare.

Acknowledgment: This work was supported in part by a grant from the Chemical Sciences, Geosciences and Biosciences Division, Office of Basic Energy Sciences, of the U. S. Department of Energy (DE-FG02-05ER15661). This work was funded by grants from the NIGMS (P41GM094091) and Hawaii Community Foundation (19ADV-95463). Funds for the upgrades of the NMR instrumentation were provided by the CRIF program of the National Science Foundation (CH E9974921) and the Elsa Pardee Foundation. The purchase of the Agilent LC−MSQTOF was funded by grant 1532310 from the MRI program of the National Science Foundation. We thank Prof. Yoshito Kishi for providing the absorption spectrum of tolyporphin A *O,O*-diacetate from the notebook of coworker Dr. W. Wang (personal communication 01/14/2015 and 07/07/2017). We thank Prof. Thomas G. Minehan for providing the absorption spectrum of the diastereomer of tolyporphin A *O,O*-diacetate. We thank Wesley Y. Yoshida for his assistance with NMR spectroscopy, and Casey Philbin for his assistance with culturing the HT-58-2 strain.

REFERENCES

1 G. M. L. Patterson, C. L. Baldwin, C. M. Bolis, F. R. Caplan, H. Karuso, L. K. Larsen, I. A. Levine, R. E. Moore, C. S. Nelson, K. D. Tschappat, G. D. Tuang, E. Furusawa, S. Furusawa, T. R. Norton and R. B. Raybourne, *J. Phycol.*, 1991, **27**, 530–536.

2 M. R. Prinsep, F. R. Caplan, R. E. Moore, G. M. L. Patterson and C. D. Smith, *J. Am. Chem. Soc.*, 1992, **114**, 385–387.

3 M. Taniguchi and J. S. Lindsey, *Chem. Rev.*, 2017, **117**, 344–535.

4 C. Brückner, *Photochem. Photobiol.,* 2017, **93**, 1320–1325.

5 Y. Zhang, R. Zhang, R.-A. Hughes, J. Dai, J. R. Gurr, P. G. Williams, E. S. Miller and J. S. Lindsey, *Phytochem. Anal.*, 2018, **29**, 205–216.

6 D. Hood, D. M. Niedzwiedzki, R. Zhang, Y. Zhang, J. Dai, E. S. Miller, D. F. Bocian, P. G. Williams, J. S. Lindsey and D. Holten, *Photochem. Photobiol.*, 2017, **93**, 1204–1215.

7 R.-A. Hughes, Y. Zhang, R. Zhang, P. G. Williams, J. S. Lindsey and E. S. Miller, *Appl. Environ. Microbiol.*, 2017, **83**, e01068-17.

8 R.-A. Hughes, X. Jin, Y. Zhang, R. Zhang, S. Tran, P. G. Williams, J. S. Lindsey and E. S. Miller, *Microbiol.,* 2018, **164**,1229–1239.

9 C. D. Smith, M. R. Prinsep, F. R. Caplan, R. E. Moore and G. M. L. Patterson, *Oncol. Res.*, 1994, **6**, 211–218.

10 M. R. Prinsep, T. G. Appleton, G. R. Hanson, I. Lane, C. D. Smith, J. Puddick and D. P. Fairlie, *Inorg. Chem*., 2017, **56**, 5577–5585.

11 P. Morlière, J.-C. Maziere, R. Santus, C. D. Smith, M. R. Prinsep, C. C. Stobbe, M. C. Fenning, J. L. Golberg and J. D. Chapman, *Cancer Res.*, 1998, **58**, 3571–3578.

12 M. R. Prinsep, G. M. L. Patterson, L. K. Larsen and C. D. Smith, *Tetrahedron*, 1995, **51**, 10523–10530.

13 M. R. Prinsep, G. M. L. Patterson, L. K. Larsen and C. D. Smith, *J. Nat. Prod.*, 1998, **61**, 1133–1136.

14 J. R. Gurr, J. Dai, C. S. Philbin, H. T. Sartain, T. J. O'Donnell, W. Y. Yoshida, W. Y. A. L. Rheingold and P. G. Williams, *J. Org. Chem*., 2020, **85**, 318–326.

15 J. A. S. Cavaleiro, J. P. C. Tomé and M. A. F. Faustino, *Top. Heterocycl. Chem.*, 2007, **7**, 179–248.

16 J. Puddick and M. R. Prinsep, *Chem. New Zealand*, 2008, **72**, 68–71.

17 K. Tidgewell, B. R. Clark, W. H. Gerwick, in *Comprehensive Natural Products II Chemistry and Biology*, Vol. 2, eds. L. Mander and W.-H. Lui, Elsevier, Oxford, 2010, pp. 141–188.

18 R. K. Singh, S. P. Tiwari, A. K. Rai and T. M. Mohapatra, *J. Antibiotics*, 2011, **64**, 401–412.

19 S. I. Elshahawi, K. A. Shaaban, M. K. Kharel and J. S. Thorson, *Chem. Soc. Rev.*, 2015, **44**, 7591–7697.

20 J.-E. Thrane, M. Kyle, M. Striebel, S. Haande, M. Grung, T. Rohrlack and T. Andersen, *PLoS One,* 2015, **10**: e0137645.

21 R. Rippka, J. Deruelles, J. B. Waterbury, M. Herdman and R. Y. Stanier, R. *J. Gen. Microbiol.*, 1979, **111**, 1−61.

22 M. R. Prinsep and J. Puddick, *Phytochem. Anal.*, 2011, **22**, 285–290.

23 L. Anderson and C. L. Hunter, *Mol. Cell. Proteom.*, 2006, **5**, 573–588.

24 M. Pellegrini, E. Marchei, S. Rossi, F. Vagnarelli, A. Durgbanshi, O. García-Algar, O. Vall and S. Pichini, *Rapid Commun. Mass Spectrom.,* 2007, **21**, 2693–2703.

25 T. G. Minehan and Y. Kishi, *Angew. Chem. Int. Ed.*, 1999, **38**, 923–925.

26 W. Wang and Y. Kishi, *Org. Lett.*, 1999, **1**, 1129–1132.

27 T. G. Minehan, Ph.D. Thesis, Harvard University, 1998.

28 M. Taniguchi, J. S. Lindsey, D. F. Bocian and D. Holten, *J. Photochem. Photobiol. C: Photochem. Rev.*, 2021, **46**, 100401.

29 J. H. C. Smith and A. Benitez, in *Modern Methods of Plant Analysis*, Vol. 4, eds. K. Paech and M. V. Tracey. Springer-Verlag: Berlin-Göttingen-Heidelberg, Germany, 1955, pp. 142–196.

30 H. H. Strain and W. A. Svec, in *The Chlorophylls*, eds. L. P. Vernon and G. R. Seely, Academic Press: New York, NY, USA, 1966, pp. 21−66.

31 U. Eisner and R. P. Linstead, *J. Chem. Soc.*, 1955, 3749–3754.

32 J. D. Keegan, A. M. Stolzenberg, Y. C. Lu, R. E. Linder, G. Barth, A. Moscowitz, E. Bunnenberg and C. Djerassi, *J. Am. Chem. Soc.*, 1982, **104**, 4305–4317.

33 S. Neya and N. Funasaki, *Tetrahedron Lett.*, 2002, **43**, 1057–1058.

34 U. Eisner, A. Lichtarowicz and R. P. Linstead, *J. Chem. Soc.*, 1957, 733–739.

35 R. Bonnett, R and G. F. Stephens, *J. Org. Chem.,* 1965, **30**, 2791–2798.

36 H. Higuchi, M. Shinbo, M. Usuki, M. Takeuchi, Y. Hasegawa, K. Tani and J. Ojima, *Bull. Chem. Soc. Jpn.*, 1999, **72**, 1887–1898.

37 A. M. Stolzenberg, P. A. Glazer and B. M. Foxman, *Inorg. Chem.*, 1986. **25**, 983–991.

38 R. Bonnett, R., M. J. Dimsdale and G. F. Stephens, *J. Chem. Soc., C*, 1969, 564–570.

39 D. B. Papkovsky, G. V. Ponomarev, W. Trettnak and P. Oleary, *Anal. Chem.*, 1995, **67**, 4112–4117.

40 R. D. Arasasingham, A. L. Balch and M. M. Olmstead, *Heterocycles,* 1988, **27**, 2111–2117.

41 P. Iakovides and K. M. Smith, *Tetrahedron,* 1996, **52**, 1123–1148.

42 U. Eisner and R. P. Linstead, *J. Chem. Soc.*, 1955, 3742–3749.

43 M. Taniguchi, M. Ptaszek, B. E. McDowell and J. S. Lindsey, *Tetrahedron*, 2007, **63**, 3840–3849.

44 H. H. Inhoffen and W. Nolte, *Liebigs Ann. Chem.*, 1969, **725**, 167–176.

45 A. R. Morgan, G. M. Garbo, R. W. Keck, D. Skalkos and S. H. Selman, *J. Photochem. Photobiol. B*, 1990, **6**, 133–141.

46 R. K. Pandey, M. Isaac, I. MacDonald, C. J. Medforth, M. O. Senge, T. J. Dougherty and K. M. Smith, *J. Org. Chem.*, 1997, **62**, 1463–1472.

47 C. K. Chang and W. Wu, *J. Org. Chem.*, 1986, **51**, 2134–2137.

48 M. Taniguchi and J. S. Lindsey, *Photochem. Photobiol.*, 2018, **94**, 290–327.

49 T. G. Minehan, L. Cook-Blumberg, Y. Kishi, M. R. Prinsep and R. E. Moore, *Angew. Chem. Int. Ed.*, 1999, **38**, 926–928.

50 M. Taniguchi, H. Du and J. S. Lindsey, *Photochem. Photobiol.*, 2018, **94**, 277–289.

51 M. Taniguchi and J. S. Lindsey, *Photochem. Photobiol.*, 2021, **97**, 136–165.

52 Y. Guo, Z. Xu, A. E. Norcross, M. Taniguchi and J. S. Lindsey, *Proc. SPIE*, 2019, **10893**, 108930O. DOI: 10.1117/12.2508077

53 M. Taniguchi and J. S. Lindsey, *Proc. SPIE*, 2020, **11256**, 112560J. DOI: 10.1117/12.2542859

54 S. M. Kupchan, R. W. Britton, M. F. Ziegler and C. W. Sigel, *J. Org. Chem.*, 1973, **38**, 178–179.

55 S. M. Kupchan, R. W. Britton, J. A. Lacadie, M. F. Ziegler and C. W. Sigel, *J. Org. Chem.*, 1975, **40**, 648–654.